Collision between magnetically trapped NH molecules in the $(N=0,J=1)$ state

Masatoshi Kajita
National Institute of Information and Communications Technology, 4-2-1 Nukui-Kitamachi, Koganei-Shi, Tokyo 184-8795, Japan
(Received 16 May 2006; published 27 September 2006)

Elastic and inelastic collisions between NH molecules in the $(N=0,J=1)$ state were analyzed. These analyses showed that the elastic collision is caused mainly by electric dipole-induced dipole interaction, and the inelastic collision is caused mainly by the magnetic dipole-dipole interaction. The collision cross sections obtained by the quantum and classical methods are roughly in good agreement in the kinetic-energy region of 5–500 mK. Moreover, the ratio of the inelastic-collision rate to the elastic-collision rate is lower than 1/200. These results show that the NH molecule is advantageous to perform evaporative cooling.

DOI: 10.1103/PhysRevA.74.032710 PACS number(s): 34.50.Ez

I. INTRODUCTION

Cold polar molecules have recently become an attractive subject for researchers (see the review in Ref. [1]), since it can realize dilute quantum gases of fermions [2–6] or bosons [7–12]. DeMille proposed using them as the qubits of a scalable quantum computer [13]. The molecular vibrational-rotational transitions can be the basis of the frequency standard in the infrared region. This would make it possible to observe the temporal change of the mass ratio of electron and proton.

Cold molecules have actually been obtained by combining laser-cooled atoms, by cooling molecules through collisions with cold gas, or by obtaining a slow molecular beam. The former method has been done using photoassociation or Feshbach resonance. Kerman *et al.* produced ultracold $RbCs^*$ molecules through photoassociation [14]. Using Feshbach resonance, Inouye *et al.* [15] produced cold KRb molecules and Stan *et al.* [16] produced cold LiNa molecules. Although molecules constructed with photoassociation or Feshbach resonance are mostly in excited states, RbCs molecules in an absolute ground state have also been produced [17,18].

Molecular cooling through collisions with cold gas has also been developed since 1997. Using a static magnetic field, a Harvard group trapped CaH molecules that were precooled through collisions with helium vapor [19,20]. It has also been proposed to cool trapped molecules (by the methods discussed below) through collisions with laser-cooled atoms [21].

Several methods have been developed to obtain slow molecular beams. To load polar molecules into a trapping area, a deceleration method using a time-varying electric field has been developed [22–25]. Bethlem *et al.* loaded decelerated ND_3 molecules into a space enclosed by quadrupole electrodes [26] and Crompvoets *et al.* loaded them into a space enclosed by ring electrodes [27]. Van de Meerakker *et al.* trapped OH molecules in a quadrupole electrode by using the same method [28]. Junglen *et al.* constructed a quadrupole guide for selecting slow molecules from a continuous molecular beam [29]. Rieger *et al.* loaded ND_3, CH_3Cl, and CH_2O molecules selected by this quadrupole guide into an electric trap [30]. A counter-rotating beam source [31,32] or billiardlike collisions in crossed beams [33] can also be used to obtain a slow molecular beam. Enomoto *et al.* proposed to decelerate polar molecules by using a microwave traveling wave [34].

By using dc electric or magnetic fields, only molecules in the low-field seeking states (cannot be the absolute ground state) can be trapped. Via the Majorana transition [35] or the inelastic collision [36–43], trapped molecules can be transformed to high-field seeking states and repelled from the traps. It is preferable to trap molecules in an absolute ground state, where inelastic collisions are not possible at ultralow temperatures. Using an ac electric field inside an octopole electrodes system, van Veldhoven *et al.* succeeded in trapping para-ND_3 molecules in the absolute ground state[44]. DeMille proposed to trap ultracold polar molecules in the absolute ground state by using a standing electromagnetic field in a microwave cavity [45].

Doyle *et al.* are planning to trap NH molecules in the $^3\Sigma$ state using the interaction between the electron spin and the magnetic field [46]. The trap loss is caused by the change of the electron-spin direction, induced by the spin-rotation interaction or by the magnetic dipole-dipole interaction between colliding molecules. The rate of collision loss is much lower than that for the elastic collision, caused by the electric dipole-induced dipole interaction. Therefore, NH molecules seem to be advantageous to perform evaporative cooling.

In the rest of this paper, elastic- and inelastic-collision cross sections are theoretically estimated by using quantum (i.e., solutions to the Schrödinger equation, Born approximation, and distorted-wave Born approximation) and classical methods. These estimations found that the inelastic-collision rate is less than 1/200 of the elastic-collision rate with kinetic energy 10^{-6}–10 K.

II. ZEEMAN SHIFT

The rotational constant of an NH molecule B_0 is so large, i.e., 490 GHz [47] and NH molecules cooled (<1 K) by cold buffer gas are mostly in the $N=0$ state, where N is the quantum number of the molecular rotation. The energy state of NH molecules in a field-free space is described by

$$J = N + S,$$

$$F_1 = J + I_H,$$

$$F = F_1 + IN,$$

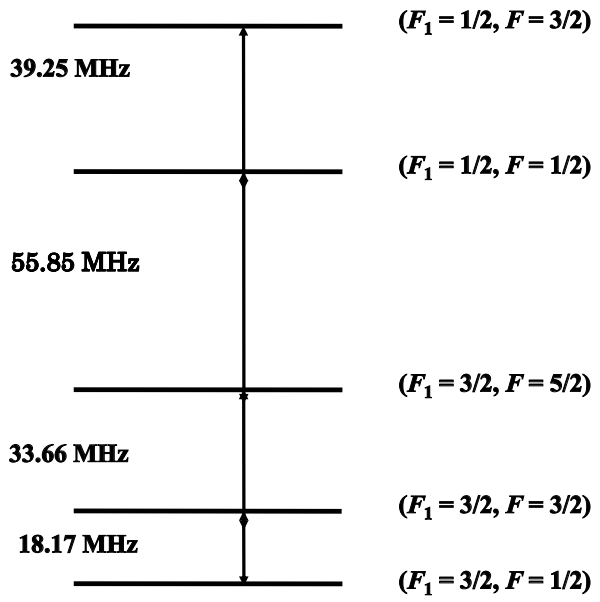

FIG. 1. Hyperfine state of ^{14}NH molecules in the $|N=0,J=1\rangle$ state.

where $S(=1)$ denotes the electron spin. $I_H(=1/2)$ and $I_N(=1$ for ^{14}N and 1/2 for ^{15}N) are the nuclear spins of H and N atoms, respectively. Figure 1 shows the hyperfine structure of the ^{14}NH molecule in the $|N=0,J=1\rangle$ state [47]. When a magnetic field is applied, energy splittings occur between degenerated sublevels $M_F=-F\sim F$, where M_X denotes the trajectories of $X(X=N,S,I_H,I_N,F)$ parallel to the magnetic field. When $N=M_N=0$, each $|F_1,F,M_F\rangle$ state is described by

$$|F_1,F,M_F\rangle = \sum c_\alpha |M_S,M_{I_H},M_{I_N}\rangle,$$

$$M_F = M_S + M_{I_H} + M_{I_H},$$

and the linear Zeeman-shift coefficients are given by

$$\sum |c_\alpha|^2 [g_S M_S + g_I(H) M_{I_H} + g_I(N) M_{I_N}]\mu_B,$$

where μ_B is the Bohr magneton, g_S is the g factor of the electron spin, and g_I is the nuclear g factor. With any magnetic field, the following relations hold and the Zeeman shift is strictly linear.

^{14}NH,

$$|N=0,J=1,F_1=3/2,F=5/2,M_F=\pm 5/2\rangle = \left|N=0,J=1,M_S=\pm 1,M_{I_H}=\pm\frac{1}{2},M_{I_N}=\pm 1\right\rangle.$$

Linear Zeeman-shift coefficient,

$$\pm\mu_B\left[g_S+\frac{1}{2}g_I(H)+g_I(N)\right].$$

^{15}NH,

$$|N=0,J=1,F_1=3/2,F=2,M_F=\pm 2\rangle = \left|N=0,J=1,M_S=\pm 1,M_{I_H}=\pm\frac{1}{2},M_{I_N}=\pm\frac{1}{2}\right\rangle.$$

Linear Zeeman-shift coefficient,

$$\pm\mu_B\left[g_S+\frac{1}{2}g_I(H)+\frac{1}{2}g_I(N)\right].$$

Actually, $g_S(=2.0031745)\gg g_I(=5.4\times 10^{-4})$ and the influences of the nuclear spins are ignored in the following discussions. When $g_S\mu_B B$ (B: magnetic field strength) is much larger than the hyperfine splittings, M_S becomes deterministic for all hyperfine states. Figure 2 shows the Zeeman shifts of ^{14}NH molecules in the $|N=0,J=1\rangle$ states. For ^{14}NH molecules in the $|N=0,J=1\rangle$ state, the following hyperfine states converge to the $M_S=1,0,-1$ states with a magnetic field higher than 40 G.

$M_S=1$,

$$\left|F_1=\frac{1}{2},F=\frac{3}{2},M_F=\frac{3}{2},\frac{1}{2},-\frac{1}{2}\right\rangle,\quad \left|F_1=\frac{1}{2},F=\frac{1}{2},M_F=\frac{1}{2}\right\rangle,$$

$$\left|F_1=\frac{3}{2},F=\frac{5}{2},M_F=\frac{5}{2},\frac{3}{2}\right\rangle.$$

$M_S=0$,

$$\left|F_1=\frac{1}{2},F=\frac{3}{2},M_F=-\frac{3}{2}\right\rangle,\quad \left|F_1=\frac{1}{2},F=\frac{1}{2},M_F=-\frac{1}{2}\right\rangle,$$

$$\left|F_1=\frac{3}{2},F=\frac{5}{2},M_F=\frac{1}{2},-\frac{1}{2}\right\rangle,\quad \left|F_1=\frac{3}{2},F=\frac{3}{2},M_F=\frac{3}{2},\frac{1}{2}\right\rangle.$$

$M_S=-1$,

$$\left|F_1=\frac{3}{2},F=\frac{5}{2},M_F=-\frac{3}{2},-\frac{5}{2}\right\rangle,$$

$$\left|F_1=\frac{3}{2},F=\frac{3}{2},M_F=-\frac{1}{2},-\frac{3}{2}\right\rangle,$$

$$\left|F_1=\frac{3}{2},F=\frac{1}{2},M_F=\frac{1}{2},-\frac{1}{2}\right\rangle.$$

If dc magnetic field is used, only molecules in the $M_S=1$ (low-field seeking) states are trapped. In this paper, assuming that the magnetic field is high enough so that M_S is a deterministic value, we discuss the collision between NH molecules in the $|N=0,J=1,M_S=1\rangle$ state. When there is a transition to the $M_S=0$ state, the molecule cannot be trapped by the magnetic field further so trap loss is caused.

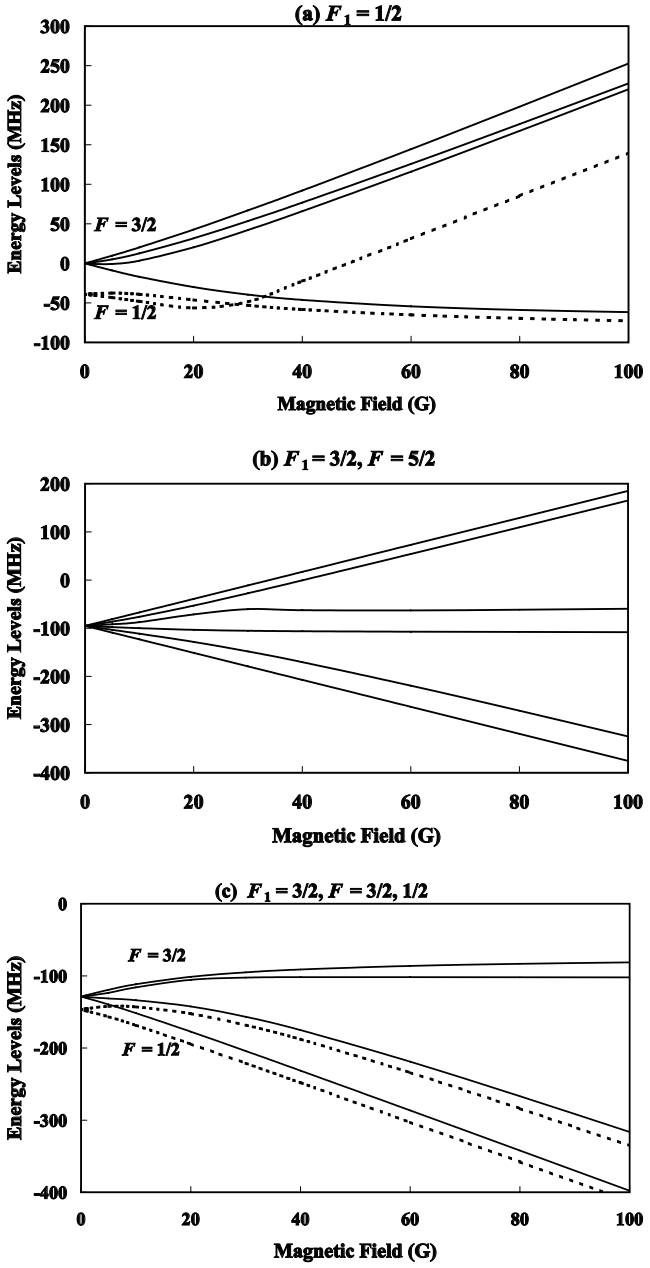

FIG. 2. Zeeman shifts of ^{14}NH molecules in the $|N=0,J=1\rangle$ state as functions of the magnetic field: (a) shows the $|F_1=1/2,F=3/2,1/2\rangle$ states, (b) shows the $|F_1=3/2,F=5/2\rangle$ state, and (c) shows the $|F_1=3/2,F=3/2,1/2\rangle$ states.

III. COLLISION

The collision cross sections are obtained from

$$\sigma = \frac{\eta(L)\pi}{k^2} \sum_{L,M_L} P(L,M_L), \tag{1}$$

where k is the incident wave number, L is the quantum number of the relative motion, M_L is its trajectory parallel to the magnetic field, P denotes the probability of the scattering of each partial wave, and $\eta(L)$ denotes the values shown below.

Collision between same boson isotopes,

$$\eta(L) = 2 \quad \text{for } L = \text{even},$$

$$\eta(L) = 0 \quad \text{for } L = \text{odd}.$$

Collision between same fermion isotopes,

$$\eta(L) = 2 \quad \text{for } L = \text{odd},$$

$$\eta(L) = 0 \quad \text{for } L = \text{even}.$$

Collision between different isotopes,

$$\eta(L) = 1.$$

Actually, the total collision cross sections should be obtained taking $L=0-L_{\max}$ into account, where $L_{\max}$ is the value that satisfies $P(L \geq L_{\max}) \ll P(L < L_{\max})$. With ultralow kinetic energy ($a \ll 1/k$, where a is the scale size of the intermolecular interaction), the total collision cross section is calculated by taking only a few partial waves into account. When the kinetic energy is high ($a \gg 1/k$), however, the contributions from many partial waves must be taken into account. Given this condition, $P(L) \approx P(L \pm 1)$ and Eq. (1) is rewritten using the impact parameter $b(=L/k)$ as

$$\sigma = 2\pi \int P(b)db. \tag{2}$$

A. Elastic collision

Although an NH molecule has an electric permanent-dipole moment $\mu_0(\sim 1.6$ D) [48], the electric diagonal-dipole matrix elements $\langle \Psi | \vec{\mu}_e | \Psi \rangle$ are zero in a field-free space and the elastic collision is not caused by the electric dipole-dipole interaction. Also, if $\langle \Psi | \vec{\mu}_e | \Psi \rangle (\propto \mu_0^2 E/hB_0)$ is induced by getting electric field E lower than 50 kV/cm, the electric dipole-dipole interaction is much smaller than the electric dipole-induced dipole interaction because of the large value of $B_0(\sim 490$ GHz). As shown later, the electric dipole-dipole interaction is significant only for the collision between the same fermion isotopes with ultralow kinetic energy.

We consider the electric dipole-induced dipole interaction, which is given by

$$H_{D\text{-}ID}(r) = -\frac{\beta}{r^6},$$

$$\beta = \frac{\mu_0^4}{96\pi^2\varepsilon_0^2 hB_0}(1 + 3\cos^2\xi), \tag{3}$$

where ξ is the angle between the relative position vector and the dipole moment vector.

1. Ultralow kinetic energy

To discuss the collision caused by the dipole-dipole interaction, the Born approximation was used to obtain $P(L,M_L)$ in Refs. [37,38,43]. However, this method cannot be used for the collision caused by the dipole-induced dipole interaction, because the integrals $\langle L=0 | H_{D\text{-}ID} | L=0 \rangle$ and $\langle L=1 | H_{D\text{-}ID} | L$

$=1\rangle$ diverge. Here, assuming $a \ll 1/k$, we consider the following solution to the Schrödinger equation [49]:

$$\frac{d^2R(r)}{dr^2} + \frac{2}{r}\frac{dR(r)}{dr} + \left[k^2 - \frac{L(L+1)}{r^2} + \frac{2m}{\hbar^2}\frac{\beta}{r^6}\right]R(r) = 0, \tag{4}$$

where m is the reduced mass. The solution of Eq. (4) with $r \gg a$ is given by

$$R_L(r) = r^L\left(\frac{d}{rdr}\right)^L \frac{\sin(kr)}{kr} - \gamma k^{2L+1} r^L \left(\frac{d}{rdr}\right)^L \frac{\cos(kr)}{kr}, \tag{5}$$

where γ is a certain parameter, determined by β. When $\beta = 0$ (without scattering), the solution to Eq. (4) is given by

$$R_L^{\text{nonscattering}}(r) = r^L\left(\frac{d}{rdr}\right)^L \frac{\sin(kr)}{(kr)}. \tag{6}$$

Comparing Eqs. (5) and (6), the scattering probability P is given by

$$P = \frac{\gamma^2 k^{4L+2}}{1 + \gamma^2 k^{4L+2}}. \tag{7}$$

When $a \ll r \ll 1/k$, Eq. (5) is rewritten as

$$R(r) = \frac{r^L}{(2L+1)!!} - \frac{(2L-1)!!\,\gamma}{r^{L+1}}. \tag{8}$$

When $L \geq 1$, $R(r)$ [see Eq. (8)] is minimum with the value of r where

$$\frac{L(L+1)}{r^2} - \frac{2m}{\hbar^2}\frac{\beta}{r^6}$$

is maximum. Therefore, γ is roughly estimated as

$$\gamma = \frac{L}{(L+1)(2L-1)!!\,(2L+1)!!}\left[\frac{6m\beta}{\hbar^2 L(L+1)}\right]^{2L+1/4}. \tag{9}$$

Each scattering term is obtained from

$$\frac{\pi}{k^2}P = \frac{\pi[L/(2L-1)!!\,(2L+1)!!\,(L+1)]^2[6m\beta/\hbar^2 L(L+1)]^{2L+1/2}k^{4L}}{1 + [L/(2L-1)!!\,(2L+1)!!\,(L+1)]^2[6m\beta/\hbar^2 L(L+1)]^{2L+1/2}k^{4L+2}},$$

with ultralow kinetic energy

$$\frac{\pi}{k^2}P \approx \pi\left[\frac{L}{(2L-1)!!\,(2L+1)!!\,(L+1)}\right]^2\left[\frac{6m\beta}{\hbar^2 L(L+1)}\right]^{2L+1/2}k^{4L},$$

with higher kinetic energy

$$\frac{\pi}{k^2}P \approx \frac{\pi}{k^2}. \tag{10}$$

When $L=0$ [50],

$$\gamma^2 = \frac{\mu_0^2}{96\varepsilon_0}\sqrt{\frac{10m}{h^3 B_0}}\frac{\Gamma^2(3/4)}{\Gamma^2(5/4)} \tag{11}$$

is obtained in the case that the wave function becomes zero at $r=0$. The $L=0$ scattering term is obtained as

$$\frac{\pi}{k^2}P = \frac{\pi\mu_0^2/96\varepsilon_0\sqrt{10m/h^3B_0}\Gamma^2(3/4)/\Gamma^2(5/4)}{1 + \mu_0^2/96\varepsilon_0\sqrt{10m/h^3B_0}\Gamma^2(3/4)/\Gamma^2(5/4)k^2}$$

with ultralow kinetic energy

$$\frac{\pi}{k^2}P \approx \frac{\pi\mu_0^2}{96\varepsilon_0}\sqrt{\frac{10m}{h^3B_0}}\frac{\Gamma^2(3/4)}{\Gamma^2(5/4)},$$

with higher kinetic energy

$$\frac{\pi}{k^2}P \approx \frac{\pi}{k^2}. \tag{12}$$

The collision cross sections between ^{14}NH (fermion) molecules and ^{15}NH (boson) molecules are shown in Fig. 3. The scattering terms $L=1,3,5$ $(0,2,4)$ were taken into account in the case of ^{14}NH (^{15}NH) molecules. The collision cross section between ^{14}NH and ^{15}NH molecules is obtained by

$$\sigma(^{14}\text{NH} - ^{15}\text{NH}) = \frac{\sigma(^{14}\text{NH} - ^{14}\text{NH}) + \sigma(^{15}\text{NH} - ^{15}\text{NH})}{2}. \tag{13}$$

2. High kinetic energy

When the kinetic energy is so high that $a \gg 1/k$ is satisfied, the collision cross section is obtained using the classical path method as shown in Eq. (4). Assuming that the relative motion is described as a straight path, Anderson derived the following formula to obtain the cross section of the collision induced by the dipole-induced dipole interaction [51]:

$$\sigma = \frac{5}{4}\pi\left[\frac{7}{960(4\varepsilon_0 h)^4}\frac{\mu_0^8}{B_0^2}\frac{m}{k_B K}\right]^{1/5}. \tag{14}$$

The elastic collision cross sections obtained with Eq. (14) are also shown in Fig. 3.

3. Intermediate kinetic energy region

The quantum treatment shown in Sec. III A 1 is based on the assumption $a \ll 1/k$, and the classical treatment shown in

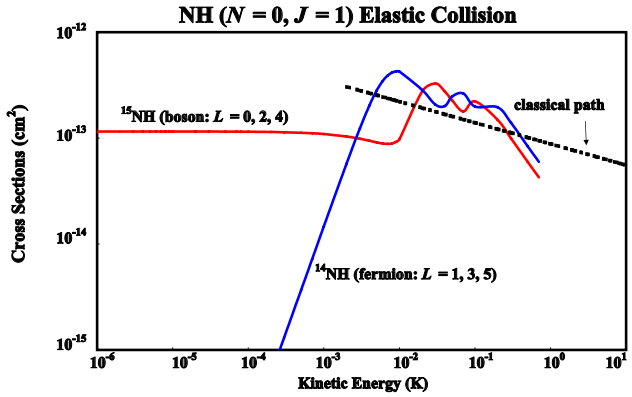

FIG. 3. (Color online) Elastic-collision cross sections between ^{14}NH (fermion) molecules and between ^{15}NH (boson) molecules as functions of the kinetic energy, when the magnetic field is 50 G. Solid lines show the results obtained by solving the Schrödinger equation taking $L=1,3,5$ for ^{14}NH molecules (online blue) and $L=0,2,4$ for ^{15}NH molecules (online red). The dotted line shows the results obtained using the classical path method.

Sec. III A 2 is valid with $a \gg 1/k$. When $a \approx 1$ nm, these assumptions are satisfied with $K/k_B < 1$ mK for the quantum method and $K/k_B > 1$ K for the classical path method. However, we use both of these methods in the case of the kinetic-energy region between 1 mK and 1 K. Figure 3 shows that the cross sections obtained using both methods are roughly in good agreement within a factor of 1.5. Equation (14) shows that the elastic collision cross section is proportional to $K^{-1/5}$, which is also obtained by the quantum treatment with $10 < K/k_B < 500$ mK. With kinetic energy higher than 500 mK, $P(L \leq 5) \approx 1$ and scattering terms $L \geq 6$ become significant. Therefore, cross sections obtained by the quantum treatment considering the scattering terms $L \leq 5$ are much smaller than those obtained by the classical path method.

B. Inelastic collision

The collision loss is caused by the $M_S = 1 \rightarrow 0, -1$ transition. For the collision between molecules in the $N \geq 1$ states, this collisional transition is caused mainly by the spin-rotation interaction. However, the spin-rotation interaction term vanishes for molecules in the pure $N=0$ state. Only when the mixture between different rotational states is significant, the spin-rotation interaction works also for the molecules in the $N=0$ state. The mixture between different rotational states is determined by $\eta = (\lambda_S / B_0)$, where λ_S is the spin-interaction constant [52]. Krems shows that the inelastic collision cross section between molecules in the $N=0$ state is almost proportional to η^4 [53]. If the inelastic collision between NH molecules is dominated by the spin-rotation interaction, the inelastic collision is expected to be five orders smaller than that between $^{17}O_2$ molecules, because of $\eta(\mathrm{NH})/\eta(\mathrm{O_2}) = 0.045$. In comparison with the calculation of the inelastic collision between $^{17}O_2$ molecules in the $N=0$ state [54], the inelastic collision between NH molecules is expected to be much smaller than 10^{-20} cm^2 when $K/k_B < 1$ mK (when $K/k_B \approx 1$ K, 10^{-19} cm^2). Krems *et al.* have concluded that the direct transitions due to the magnetic-dipole interaction dominates the inelastic collision between the molecules in the $N=0$ state [52], comparing their own calculations [53] and the experimental measurements for spin relaxation in the He-CaH($^2\Sigma$) collisions [19].

Therefore, we consider the cross section of the $M_S = 1 \rightarrow 0$ transition caused by the magnetic dipole-dipole interaction, which is given by

$$H_{DD} = \frac{1}{4\pi\varepsilon_0 c^2 r^3}\left[\vec{\mu}_{m1}\cdot\vec{\mu}_{m2} - \frac{3(\vec{\mu}_{m1}\cdot\vec{r})(\vec{\mu}_{m2}\cdot\vec{r})}{r^2}\right], \tag{15}$$

where $\vec{\mu}_{m1,2}$ is the magnetic-dipole moment vector. The inelastic-collision cross sections were obtained using the magnetic-dipole matrix elements

$$|\langle M_S = 0|\vec{\mu}_m|M_S = 1\rangle| = |\langle M_S = 1|\vec{\mu}_m|M_S = 1\rangle| = \frac{g_S}{\sqrt{2}}\mu_B. \tag{16}$$

The inelastic-collision cross sections were calculated using the Born approximation (BA), distorted-wave Born approximation (DWBA), and the classical path method.

1. Born approximation

The Born approximation is the simplest method to estimate the collision cross sections with ultralow kinetic energy. With the BA, it is assumed that the collision interaction is so weak that the distortion of the wave function is negligible. All scattering terms of the $|\Phi_{i1},\Phi_{i2}\rangle \rightarrow |\Phi_{f1},\Phi_{f2}\rangle$ transition are thus given by

$$\frac{\pi}{k^2}P[|\Phi_{i1},\Phi_{i2}\rangle \rightarrow |\Phi_{f1},\Phi_{f2}\rangle,(L,M_L)\rightarrow(L',M_L')] = \frac{m^2}{4\pi\varepsilon_0^2\hbar^4}G_{L,L'}\left(\frac{k'}{k}\right) \times F(\Delta M_{S1},\Delta M_{S2},L,M_L,L',M_L'),$$

$$G_{L,L'}\left(\frac{k'}{k}\right) = \frac{k'}{k}\left[\int_0^\infty Q_L^*(kr)\frac{1}{r}Q_{L'}(k'r)dr\right]^2,$$

$$Q_L(r) = R_L^{\text{non-scattering}}(r) = r^L\left(\frac{d}{rdr}\right)^L\frac{\sin(kr)}{(kr)},$$

$$\frac{k'}{k} = \sqrt{1+\frac{\Delta E}{K}}, \tag{17}$$

where k' denotes the wave number of the scattered wave, ΔE is the change of the total internal states of molecules caused by the inelastic collision, and F is an operator. When $k \ll k'(K \ll \Delta E)$, the inelastic-collision cross section is proportional to $K^{1/2}$ and $K^{-1/2}$ for the ^{14}NH molecule (fermion) and the ^{15}NH molecule (boson), respectively [38]. When $k \approx k'$ $(K \gg \Delta E)$, the inelastic-collision cross section has no depen-

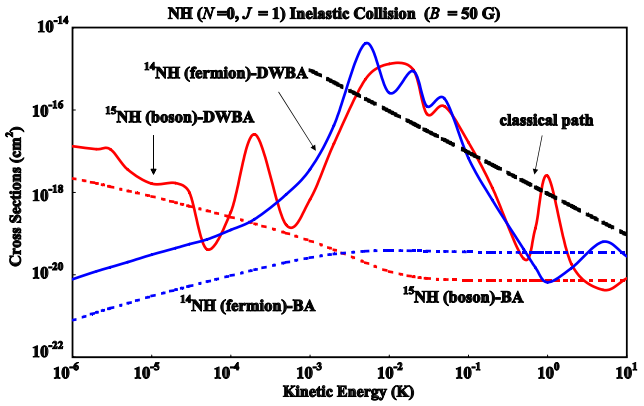

FIG. 4. (Color online) Inelastic collision cross sections between ^{14}NH (fermion) molecules and between ^{15}NH (boson) molecules as functions of the kinetic energy, when the magnetic field is 50 G. The dotted and solid lines show the cross sections obtained using the Born approximation (BA) and distorted-wave Born approximation (DWBA), respectively. For ^{14}NH (fermion) molecules, $L=1 \rightarrow 1$ was taken into account (online blue). For ^{15}NH (boson) molecules, $L=0,2 \rightarrow 2,0$ were taken into account (online red). The cross section obtained by the classical path method is also shown with a dashed line.

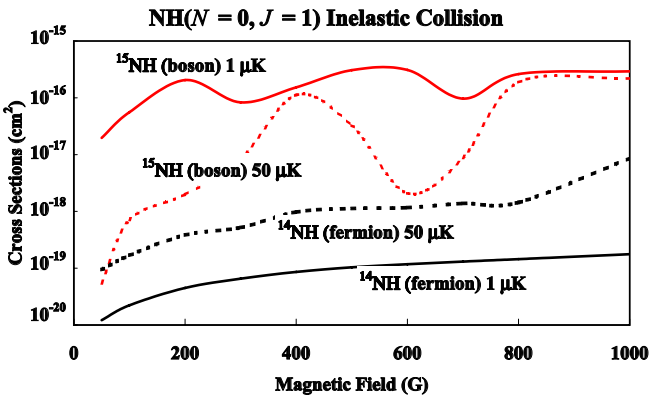

FIG. 5. (Color online) Inelastic-collision cross sections between ^{14}NH (fermion) molecules and between ^{15}NH (boson) molecules as functions of the magnetic field, taking the kinetic energy of 1 and 50 μK. For ^{14}NH (fermion) molecules, $L=1 \rightarrow 1$ was taken into account (online black). For ^{15}NH (boson) molecules, $L=0,2 \rightarrow 2,0$ were taken into account (online red).

dence on K. The calculation was performed taking $L=1 \rightarrow 1$ for a ^{14}NH molecule and $L=0,2 \rightarrow 2,0$ for a ^{15}NH molecule into account. When the BA is used, the scattering terms are independent on K at the kinetic-energy region lower than 10^4 K. Therefore, the contribution of higher L terms cannot be significant at a kinetic energy lower than 10 K.

2. Distorted-wave Born approximation

The wave function is distorted by the intermolecular interaction. The distorted-wave Born approximation takes the distortion of wave functions caused by the electric dipole-induced dipole interaction into account. The calculation is performed using Eq. (17), taking

$$Q_L(r) = R_L(r) = r^L \left(\frac{d}{rdr}\right)^L \frac{\sin(kr)}{(kr)} - \gamma k^{2L+1} r^L \left(\frac{d}{rdr}\right)^L \frac{\cos(kr)}{(kr)}, \quad r \geq d$$

$$Q_L(kr) = 0, \quad r < d, \tag{18}$$

where d denotes the area where the intermolecular exchange (repulsive force) is significant. If we do not take a nonzero value of d, $G(k'/k)$ diverges.

Figure 4 shows the inelastic-collision cross sections between ^{14}NH (fermion) and between ^{15}NH (boson) molecules, obtained using the BA and the DWBA with $B=50$ G and $d=0.35$ nm. Given $K/k_B < 100$ μK, the proportionality between the inelastic-collision cross sections and $K^{1/2}$ ($K^{-1/2}$) was also obtained from the DWBA for the collision between ^{14}NH(^{15}NH) molecules. The value of the inelastic-collision cross sections obtained by the DWBA is larger than that obtained by the BA with a factor of 10 [Eq. (6)] for the collision between ^{14}NH(^{15}NH) molecules. This result is derived in Appendix A. References [41,42] show that the inelastic-collision cross sections between polar molecules in the $^1\Sigma$and $^2\Pi$ states obtained by the close-coupling method is almost one order larger than those obtained by the BA.

When the kinetic energy becomes higher than 1 mK, the inelastic-collision cross section obtained by the DWBA increases significantly. This is because the distortion of the wave function becomes significant ($\gamma k^{2L+1} \geq 0.1$). This phenomenon has not been obtained before with electric dipole-dipole interaction, because P converges to 1 when the kinetic energy is so high that the distortion of the wave function is significant.

Figure 5 shows the inelastic-collision cross sections obtained by the DWBA as a function of the magnetic field when $K/k_B=1$ and 50 μK. If the BA is valid, the inelastic collision should be proportional to $\Delta E^{-1/2}$ and $B^{-1/2}$($\Delta E^{1/2}$ and $B^{1/2}$) for ^{14}NH(^{15}NH) molecules. As shown in Appendix A, this proportionality is not valid when the DWBA is used with $\gamma k'^{2L'+1} \geq 1$ (distortion of the scattering wave is significant).

3. Classical path method

When the kinetic energy is so high that $a \gg 1/k$ is satisfied, the collision cross section is obtained by using the classical path method as shown in Eq. (2). For dipole-dipole interaction, $P(b)$ is obtained by [55]

$$P(b) = \min[1, S(d), S(b)],$$

$$S(b) = \frac{2\pi^2 m g_S^4 \mu_B^4}{9h^2 k_B K b^4} \exp[-\lambda b^2],$$

$$\lambda = \frac{16}{3} \frac{m}{2k_B K} \left(\frac{\Delta E}{h}\right)^2. \tag{19}$$

Taking $d=0.35$ nm, $S(d) \ll 1$. Under the assumption that $\Delta E/k_B < 1$ K and $K/k_B > 0.2$ K, $\lambda b^2 < 1$ with $b=d$ and the

difference of the collision cross sections when $\Delta E/k_B=0$ and 1 K is less than 1%. With the two collision channels $(M_S=1,M_S=1)\rightarrow(M_S=1,M_S=0)$ and $(M_S=0,M_S=0)$ taken into consideration, the inelastic-collision cross section is given by

$$\sigma = 2\times 2\pi d^2 S(d) = \frac{8\pi^3 m g_S^4 \mu_B^4}{9h^2 k_B K d^2}. \tag{20}$$

Figure 4 also shows the inelastic-collision cross sections obtained by the classical path method with $K/k_B>1$ mK.

4. Intermediate kinetic-energy region

In the kinetic-energy region between 5–500 mK, the inelastic collision cross sections obtained by the BA are 3–4 orders smaller than those obtained by the DWBA or the classical path method. This result shows that the BA cannot be used to discuss the collision in this kinetic-energy region. When $\gamma k^{2L+1}\gg 1$, the inelastic-collision cross sections obtained using DWBA are proportional to $(Kd^2)^{-1}$ (see Appendix B), because the distorted wave functions must be localized at $r\approx d$. The same tendency is also derived from the classical path method [see Eq. (20)]. Both DWBA and the classical path method can therefore be used to describe the characteristics of the inelastic collision in the intermediates kinetic-energy region.

The inelastic-collision cross sections obtained by the DWBA are almost one order larger than those obtained by the classical path method. This discrepancy is caused by using the formula for the distorted wave, which is valid only when $a<1/k$. The collisions caused by the magnetic interaction are much more sensitive to the distortion of the wave function than those induced by electric interactions, where P converges to 1 when the distortion of the wave function is significant. To obtain accurate values of inelastic-collision cross sections with high kinetic energy, the DWBA calculation should be performed with a more accurate formula for distorted wave functions. The couplings between different hyperfine states are weak because the magnetic interaction is so weak that P is less than 10^{-4} also with $K/k_B=10$ K.

The inelastic-collision cross section in Fig. 4 decreases rapidly when the kinetic energy becomes higher than 0.5 K, which is not possible (as explained in Appendix B). This discrepancy is caused because $R(d)$ given by Eq. (18) becomes significantly lower when $kd>1$, although the actual wave function has high density at $r\approx d$.

C. Possibility of evaporative cooling

Figures 3 and 4 show that the elastic-collision cross sections between ^{14}NH (fermion) and between ^{15}NH (boson) molecules are more than two orders larger than the inelastic-collision cross sections when the kinetic energy is higher than 10 μK and 10 nK, respectively. ^{14}NH molecules are less capable of performing evaporative cooling than ^{15}NH molecules, because the elastic cross section decreases as the kinetic energy decreases ($\propto K^2$).

However, evaporative cooling of ^{14}NH molecules becomes possible also when kinetic energy is lower than 10 μK by applying an electric field, which induces the electric dipole-dipole interaction. For simplicity, we assume that the electric-field direction is parallel to the magnetic-field direction (the treatment is very complicated when the directions of electric and magnetic fields are not parallel [56]). Figure 6 shows the elastic-collision cross sections between ^{14}NH molecules with or without the electric field (50 kV/cm). The electric dipole-dipole interaction is calculated using the DWBA. The influence of the electric dipole-dipole interaction is significant when $K/k_B<10$ μK and the electric-field strength is 50 kV/cm. When the electric field is applied, evaporative cooling of ^{14}NH molecules is possible also when the temperature is lower than 10 μK, because the electric dipole-dipole interaction cannot induce collision loss.

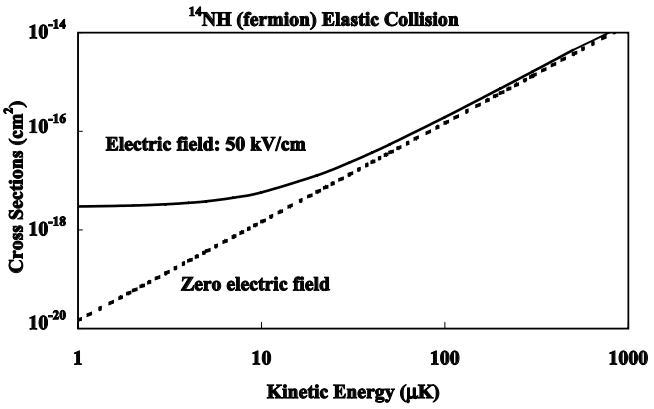

FIG. 6. Elastic-collision cross sections between ^{14}NH (fermion) molecules as a function of kinetic energy with and without electric field (50 kV/cm).

The electric field gives the mixture between $N=0$ and 1 states. Then the spin-rotation interaction becomes significant and the inelastic-collision cross section is increased. Therefore, the electric field should be given only after the molecular temperature becomes low enough, so that the spin-rotation interaction between fermion molecules is very small.

IV. CONCLUSION

We have estimated the elastic- and inelastic-collision cross sections of NH molecules in the $|N=0,J=1\rangle$ state. The elastic collision is caused by the electric dipole-induced dipole interaction, while the inelastic collision is caused by the magnetic dipole-dipole interaction (because of $N=0$ and the large value of B_0). Quantum treatment was used for the ultralow kinetic-energy region and the classical path method was used for the high kinetic-energy region. Although both calculations were performed using rather simplified formulas, the elastic-collision cross sections obtained by the quantum and classical methods are in good agreement (within a factor of 1.5) at the intermediate kinetic-energy region (5–500 mK). Moreover, for the inelastic collision, the distorted-wave Born approximation and the classical path method give the same dependence on the kinetic energy.

Elastic-collision cross sections are much larger (more than two orders) than the inelastic-collision cross sections for both ^{14}NH (fermion) and ^{15}NH (boson) molecules at tem-

peratures higher than 10 μK. Therefore, evaporative cooling is easy when the temperature is higher than 10 μK. In the lower kinetic-energy region, evaporative cooling is possible only for ^{15}NH molecules, because the elastic-collision cross section between ^{14}NH molecules becomes very small. This problem is solved by applying an electric field, which induces the electric dipole-dipole interaction.

NH molecules trapped by a magnetic field can be electrically polarized in one direction by applying a homogenous electric field. This makes it easy to study the characteristics of polar dilute quantum gases. Also note that the linear Zeeman coefficients of ^{14}NH molecules in the $|N=0,J=1,F_1=3/2,F=5/2,M_F=5/2\rangle$ state and ^{15}NH molecules in the $|N=0,J=1,F_1=3/2,F=2,M_F=2\rangle$ state do not depend on the vibrational state and the vibrational transition can be measured without the influence of the Zeeman shift. Therefore, the vibrational spectrum of cold NH molecules (3489 cm^{-1} [48]) can form the basis of a molecular clock [57]. The clock laser is applicable for the optical network, after doubling its frequency.

The estimation method of elastic-collision cross sections shown in this paper is applicable also for other molecules in the $^3\Sigma$ $N=0$ state. The spin-rotation interaction should be taken into account for inelastic collisions between molecules with a small rotational constant (the mixture between different rotational states is significant).

ACKNOWLEDGMENT

The author is very thankful to Professor J. M. Doyle for sharing their plan to trap NH molecules.

APPENDIX A

When the BA is valid, each scattering term $[\pi P(L\rightarrow L')/k^2]$ is proportional to $(K/\Delta E)^{L-1/2}$ [38], under the assumption that $k' \gg k$ ($\Delta E \gg K$). This appendix discusses the validity of this relation when the distorted-wave Born approximation (DWBA) is used. At an ultralow kinetic-energy region, $\gamma k^{2L+1} \ll 1$ is valid. However, k' is determined mainly by ΔE and $\gamma k'^{2L'+1} \geq 1$ is also possible. With $kr \gg \pi$, $R_L(kr)$ converges to

$$R_L(kr) \rightarrow \frac{\sin(kr + L\pi/2 + \delta)}{kr},$$

$$\delta = \tan^{-1}(\gamma k^{2L+1}).$$

When $k' \gg k$, $G_{L,L'}(k'/k)$ is actually determined by

$$G_{L,L'}\left(\frac{k'}{k}\right) = \frac{k'}{k}\left[\int_d^\infty R_L^*(kr)\frac{1}{r}R_{L'}(k'r)dr\right]^2 = \frac{k'}{k}\left[\int_d^{\pi/k'} R_L^*(kr)\frac{1}{r}R_{L'}(k'r)dr\right]^2.$$

When $\gamma k^{2L+1} \ll 1$ and $kr \ll \pi$, $R_L^*(kr)$ is proportional to $(kr)^L$ and

$$\int_d^{\pi/k'} R_L^*(kr)\frac{1}{r}R_{L'}(k'r)dr \propto k^L \int_d^{\pi/k'} r^{L-1}R_{L'}(k'r)dr$$

and

$$G_{L,L'}\left(\frac{k'}{k}\right) \propto k^{2L-1} \propto K^{L-1/2}$$

is also derived when the DWBA is used. Therefore, the inelastic-collision cross sections between fermion (boson) molecules are proportional to $K^{1/2}(K^{-1/2})$. With the BA, the distribution of the wave function $R_{L'}(k'r)$ becomes maximum at $k'r \approx L'$. However, it becomes a maximum with $r \approx d(<L'/k')$ when $\gamma k'^{2L'+1} \geq 1$. Therefore, the inelastic-collision cross section obtained by the DWBA is larger than that obtained by the BA. Only when $\gamma k'^{2L'+1} \ll 1$, the scattering terms are proportional also to $(1/\Delta E)^{L-1/2}$.

APPENDIX B

This appendix discusses the dependence of the cross section of the collision induced by the magnetic dipole-dipole interaction on the kinetic energy under the assumption that $k \approx k'(K \gg \Delta E)$. We discuss using the DWBA. $G_{L,L'}(k'/k)$ is given by

$$G_{L,L'}(k) = \left[\int_d^\infty R_L^*(kr)\frac{1}{r}R_{L'}(kr)dr\right]^2 = \left[\int_{kd}^\infty R_L^*(kr)\frac{1}{(kr)}R_{L'}(kr)d(kr)\right]^2 = \left|\left\langle\frac{1}{(kr)}\right\rangle_{av}\right|^2.$$

When $\gamma k^{2L+1} \ll 1$, the distribution of $|R_L(kr)|$ is maximum with $(kr) \approx L$ and $G_{L,L'}(k)$ is independent with k and K. When $\gamma k^{2L+1} \gg 1$, however, the distribution of the wave function becomes maximum at $r \approx d$ and $G_{L,L'}(k) \approx 1/(kd)^2 \propto (Kd^2)^{-1}$. Therefore, the inelastic-collision cross section obtained by the DWBA is proportional to K^{-1} when the kinetic energy is higher than 10 mK.

[1] J. Doyle, B. Friedrich, R. V. Krems, and F. Masnou-Seeuws, Eur. Phys. J. D **31**, 149 (2004).
[2] L. You and M. Marinescu, Phys. Rev. A **60**, 2324 (1999).
[3] K. Goral, B.-G. Englert, and K. Rzazewski, Phys. Rev. A **63**, 033606 (2001).
[4] M. A. Baranov, M. S. Marenko, Val S. Rychkov, and G. V. Shlyapnikov, Phys. Rev. A **66**, 013606 (2002).
[5] M. A. Baranov *et al.*, Phys. Scr., T **T102**, 74 (2002).
[6] M. A. Baranov, L. Dobrek, and M. Lewenstein, Phys. Rev. Lett. **92**, 250403 (2004).
[7] S. Yi and L. You, Phys. Rev. A **61**, 041604(R) (2000).
[8] L. Santos, G. V. Shlyapnikov, P. Zoller, and M. Lewenstein,

Phys. Rev. Lett. **85**, 1791 (2000).
[9] S. Yi and L. You, Phys. Rev. A **63**, 053607 (2001).
[10] K. Goral and L. Santos, Phys. Rev. A **66**, 023613 (2002).
[11] S. Giovanazzi, A. Gorlitz, and T. Pfau, Phys. Rev. Lett. **89**, 130401 (2002).
[12] D. H. J. O'Dell, S. Giovanazzi, and C. Eberlein, Phys. Rev. Lett. **92**, 250401 (2004).
[13] D. DeMille, Phys. Rev. Lett. **88**, 067901 (2002).
[14] A. J. Kerman, J. M. Sage, S. Sainis, T. Bergeman, and D. DeMille, Phys. Rev. Lett. **92**, 033004 (2004).
[15] S. Inouye, J. Goldwin, M. L. Olsen, C. Ticknor, J. L. Bohn, and D. S. Jin, Phys. Rev. Lett. **93**, 183201 (2004).
[16] C. A. Stan, M. W. Zwierlein, C. H. Schunck, S. M. F. Raupach, and W. Ketterle, Phys. Rev. Lett. **93**, 143001 (2004).
[17] A. J. Kerman, J. M. Sage, S. Sainis, T. Bergeman, and D. DeMille, Phys. Rev. Lett. **92**, 153001 (2004).
[18] J. M. Sage, S. Sainis, T. Bergeman, and D. DeMille, Phys. Rev. Lett. **94**, 203001 (2005).
[19] J. D. Weinstein, R. deCarvalho, T. Guillet, B. Friedrich, and J. M. Doyle, Nature (London) **395**, 148 (1998).
[20] J. M. Doyle and B. Friedrich, Nature (London) **401**, 749 (1999).
[21] W. Shoelkopf, S. Y. T. van der Meerakker, B. Friedrich, and G. Meijer (private communication).
[22] H. L. Bethlem, G. Berden, and G. Meijer, Phys. Rev. Lett. **83**, 1558 (1999).
[23] H. L. Bethlem, G. Berden, A. J. A. van Roij, F. M. H. Crompvoets, and G. Meijer, Phys. Rev. Lett. **84**, 5744 (2000).
[24] H. L. Bethlem and G. Meijer, Int. Rev. Phys. Chem. **22**, 73 (2003).
[25] M. R. Tarbutt, H. L. Bethlem, J. J. Hudson, V. L. Ryabov, V. A. Ryzhov, B. E. Sauer, G. Meijer, and E. A. Hinds, Phys. Rev. Lett. **92**, 173002 (2004).
[26] H. L. Bethlem, G. Berden, F. M. H. Crompvoets, R. T. Jongma, A. J. A. van Roij, and G. Meijer, Nature (London) **406**, 491 (2000).
[27] F. M. H. Crompvoets, H. L. Bethlem, R. T. Jongma, and G. Meijer, Nature (London) **411**, 174 (2001).
[28] S. Y. T. van de Meerakker, P. H. M. Smeets, N. Vanhaecke, R. T. Jongma, and G. Meijer, Phys. Rev. Lett. **94**, 023004 (2005).
[29] T. Junglen, T. Rieger, S. A. Rangwala, P. W. H. Pinkse, and G. Rempe, Eur. Phys. J. D **31**, 365 (2004).
[30] T. Rieger, T. Junglen, S. A. Rangwala, P. W. H. Pinkse, and G. Rempe, Phys. Rev. Lett. **95**, 173002 (2005).
[31] M. Gupta and D. Herschbach, J. Phys. Chem. A **103**, 10670 (1999).
[32] M. Gupta and D. Herschbach, J. Phys. Chem. A **105**, 1626 (2001).
[33] M. S. Elioff, J. J. Valentini, and D. W. Chandler, Eur. Phys. J. D **31**, 385 (2004).
[34] K. Enomoto and T. Momose, Phys. Rev. A **72**, 061403(R) (2005).
[35] M. Kajita, T. Suzuki, H. Odashima, Y. Moriwaki, and M. Tachikawa, Jpn. J. Appl. Phys., Part 2 **40**, L1260 (2001).
[36] M. Kajita, Eur. Phys. J. D **20**, 55 (2002).
[37] M. Kajita, Eur. Phys. J. D **23**, 337 (2003).
[38] M. Kajita, Phys. Rev. A **69**, 012709 (2004).
[39] J. L. Bohn, Phys. Rev. A **63**, 052714 (2001).
[40] A. V. Avdeenkov and J. L. Bohn, Phys. Rev. A **66**, 052718 (2002).
[41] A. V. Avdeenkov and J. L. Bohn, Phys. Rev. A **71**, 022706 (2005).
[42] A. V. Avdeenkov, M. Kajita, and J. L. Bohn, Phys. Rev. A **73**, 022707 (2006).
[43] M. Kajita, Eur. Phys. J. D **38**, 315 (2006).
[44] J. van Veldhoven, H. L. Bethlem, and G. Meijer, Phys. Rev. Lett. **94**, 083001 (2005).
[45] D. DeMille, D. R. Glenn, and J. Petricka, Eur. Phys. J. D **31**, 375 (2004).
[46] J. M. Doyle (private communication).
[47] J. F. Mijangos, J. M. Brown, F. Matsushima, H. Odashima, K. Takagi, L. R. Zink, and K. Evenson, J. Mol. Spectrosc. **225**, 189 (2004).
[48] http://webbook.nist.gov/chemistry/
[49] L. D. Landau and E. M. Lifshits, *Quantum Mechanics* (Tosho, Tokyo, 1970), p. 579 (in Japanese).
[50] L. D. Landau and E. M. Lifshits, *Quantum Mechanics* (Tosho, Tokyo, 1970), p. 584 (in Japanese).
[51] P. W. Anderson, Phys. Rev. **76**, 647 (1949).
[52] R. V. Krems and A. Dalgarno, J. Chem. Phys. **120**, 2296 (2004).
[53] R. V. Krems, A. Dalgarno, N. Balakrishnan, and G. C. Groenenboom, Phys. Rev. A **67**, 060703(R) (2003).
[54] A. V. Avdeenkov and J. L. Bohn, Phys. Rev. A **64**, 052703 (2001).
[55] M. Kajita, Eur. Phys. J. D **31**, 39 (2004).
[56] B. Friedrich and D. Herschbach, J. Chem. Phys. **111**, 6157 (1999).
[57] M. Kajita, Phys. Rev. A **74**, 035403 (2006).